SUPPLEMENTARY DATA

Methods of the supplementary data

Cardiac magnetic resonance (CMR) imaging

CMR examinations were conducted with a Philips 1.5-Tesla Achieva whole-body scanner (Philips Healthcare, Best, The Netherlands) equipped with a 32-element phased-array torso/cardiac coil. The imaging protocol included a standard segmented cine steady-state free-precession (SSFP) sequence to provide high-quality anatomical references; a T_1-weighted turbo spin echo (T_1W-TSE) sequence to assess pericardial thickness; a T_2-weighted short-tau triple inversion recovery (T_2W-STIR) sequence to assess the extent of oedema; a T_2-gradient-spin-echo mapping (T_2-GraSE map) sequence to provide precise myocardial T_2 relaxation time properties; and a T_1-modified Look-Locker imaging (T_1-MOLLI with and acquisition scheme 5 [3] 3) before and 15 minutes after contrast media administration to assess myocardial T_1-relaxation time properties and extracellular volume ratio calculation. Late gadolinium enhancement (LGE) imaging was performed using several series of T_1-weighted inversion recovery imaging acquired 10 to 15 minutes after intravenous administration of 0.15 mmol gadobutrol contrast agent per kg body weight (Gadovist, Bayer HealthCare Pharmaceuticals, United States). LGE imaging includes 3-dimensional (3D) and 2D T_1-weighted inversion recovery turbo field echo (T_1-IR-TFE) with precise selection of correct inversion time with previous Look-Locker, 3D T_1-weighted phase sensitive inversion recovery (T_1-PSIR) during expiration breath-hold, and free-breathing 3D T_1-weighted phase sensitive inversion recovery (3D-T_1-PSIR_FB_NAV) acquired with respiratory-gating to avoid breath motion artefacts. All sequences, except the last one, were acquired during expiration breath-hold mode.

The imaging parameters for each sequence were:

- SSFP cine imaging: field of view (FOV) of 320 x 320 mm, a slice thickness of 8 mm with 2 mm gap, TR 3.0 ms, TE 1.5 ms, flip angle 60°, cardiac phases 30, voxel size 2.0 x 2.0 mm^2, and 1 NEX.

- T_2W-STIR: FOV 320 x 320, slice thickness 10 mm, TR 2 heartbeats, TE 70 ms, voxel size 1.9 x 2.4 mm^2, delay 160 ms, end-diastolic acquisition, echo-train length 35, and 2 NEX.

- T_1W-TSE: FOV 320 x 320, slice thickness 8 mm with 2 mm gap, TR 1 heartbeats, TE 9 ms, voxel size 1.9 x 2.4 mm^2, delay 160 ms, end-diastolic acquisition, echo-train length 24, and 1 NEX.

- T_2-GraSE mapping: FOV 320 x 320 with an acquisition voxel size of 2.0 x 2.5 mm^2 and slice thickness 8 mm, TR 2 heartbeats, and 8 echo times ranging from 23 to 194 ms, EPI factor 7, and 1 NEX. No registration algorithm was used before estimation of T_2 maps; however, the presence of motion artefacts between different TE for each T_2 map analyzed was specifically checked.

- T_1-MOLLI mapping: scheme 5 (3) 3, FOV 320 x 320 with an acquisition voxel size of 2.0 x 2.5 mm^2 and slice thickness 8 mm, TR 2 heartbeats, TE 1 ms, flip angle 35º and 8 to 12 echo times ranging from 200 to 4000 ms precontrast and 200 to 5000 ms postcontrast, and 1 NEX. No registration algorithm was used before extimation of T_1 maps; however, the presence of motion artefacts between different TE for each T_1 map analyzed was specifically checked.

- 3D-T_1-IR-TFE: FOV 280 x 280, slice thickness 10 mm with 5 mm oversampling between slices, TR 3.0 ms, TE 1.5 ms, flip angle 14°, voxel size 2.0 x 2.3 mm^2, inversion time 250 to 350 (optimized to null normal myocardium with prior Look-Locker sequence), TFE factor 50, average 1.

- 2D-T_1-IR-TFE: FOV 280 x 250, slice thickness 10 mm with no gap, TR 6.0 ms, TE 3.0 ms, flip angle 25°, voxel size 1.6 x 1.9 mm^2, inversion time 250 to 350 (optimized to null normal myocardium with prior Look-Locker sequence), TFE factor 24, average 1.

- 3D T_1-PSIR: FOV 280 x 280, slice thickness 10 mm with 5 mm oversampling between slices, TR 5.0 ms, TE 2.0 ms, flip angle 15°, voxel size 1.9 x 2.0 mm^2, TFE factor 37, average 1.

- 3D T_1-PSIR with breath-gating: FOV 320 x 320, slice thickness 10 mm with 5 mm oversampling between slices, TR 5.0 ms, TE 2.0 ms, flip angle 25°, voxel size 1.9 x 1.9 mm2, TFE factor 30, average 1.

SSFP cine imaging was performed to acquire 12 contiguous short-axis slices covering the heart from the base to the apex, and on the 3 cardiac long-axis (2-chambers, 4-chambers, 3-chambers). T_2W-STIR, 8 contiguous short-axis slices covering the myocardium. T_1W-TSE, same slices as T_2W-STIR and 8 to 10 axial slices covering the pericardium. T_2 and T_1 maps, 3 short-axis slices at base-mid papillary muscles and mid-apical level corresponding to the same anatomical level in all acquisitions. 3D-T_1W-LGE 18 to 22 contiguous short-axis slices and 14 to 16 contiguous slices on 2-chamber and 4-chamber geometries covering the entire heart. 2D-T_1W-LGE, 10 to 12 contiguous short-axis slices covering the heart from the base to the apex.

CMR analysis CMR images were analyzed using dedicated software (IntelliSpace Portal v.6.0.5, Philips Healthcare, The Netherlands; and MedisSuite 3.2 QMass 8.1 QMap 2.2, QStrain 2.0, Medis, The Netherlands) by 2 EACVI-CMR certified readers (M.B.-P., A.M.-G), and blinded to clinical and electrocardiogram information. CMR interpretation and measures were performed according the Society of Cardiovascular Magnetic Resonance position statement "Standardized image interpretation and postprocessing in CMR – 2020 update".[1] Papillary muscles and trabecular tissue were included in the blood pool volume. Reference ranges with the same approach were used.[2]

Before T_1 and T_2 maps were read, the presence of motion artefacts between different TE for each map was specifically checked, and manual corrections between TE were made when necessary. To perform the segmental analysis according to the 16-segment American Heart Association model, endocardial and epicardial borders were manually traced, taking care to not include ventricle cavity or pericardium. A reference point to segment each short-axis slide was placed between anterior and anteroseptal segment.

For myocardial feature tracking analysis, cine images were analyzed with QStrain Medis v.2.0. Left ventricular global longitudinal strain (GLS) calculation was performed in 2-chamber, 3-chamber and 4-chamber long-axis views. In cardiac short-axis all software packages required drawing of an endo- and epicardial contour. Left ventricular global circumferential strain and

global radial strain calculation were performed on 3 preselected short-axis views at base-mid, mid and mid-apical levels. Long-axis direction required only an endocardial contour while drawing of an endo- and epicardial contour was required in short-axis. The contours were drawn on an end-systolic image with subsequent tracking of the contours over the remainder of the images. If tracking was suboptimal, the contours on the end-systolic and end-diastolic images were adapted before re-running the tracking analysis. Right ventricle RV-GLS was performed with similar methodology and only free-wall segments were included in the assessment. Finally, left atrium global longitudinal strain (LA-GLS) was performed similarly on 2-chamber views.

REFERENCES

1. Schulz-Menger J, Bluemke D, Bremerich J, et al. Standardized image interpretation and post-processing in cardiovascular magnetic resonance - 2020 update : Society for Cardiovascular Magnetic Resonance (SCMR): Board of Trustees Task Force on Standardized Post-Processing. *J Cardiovasc Magn Reson.* 2020;22:19.

2. Petersen S, Khanji M, Plean S, Lancellotti P, Bucciarelli-Ducci C. European Association of Cardiovascular Imaging Expert Consensus Paper: A Comprehensive Review of Cardiovascular Magnetic Resonance Normal Values of Cardiac Chamber Size and Aortic Root in Adults and Recommendations for Grading Severity. *Eur Heart J Cardiovasc Imaging.* 2019;20:1321-1331.

Table 1 of the supplementary data

Cardiovascular chronic drug therapy and drug therapy aimed at ameliorating COVID-19 disease.

	All participants	Presence of pericardial and myocardial manifestations				*P*
	(N = 139)	No (n = 96)	Pericarditis (n = 8)	Myopericarditis (n = 11)	Myocarditis (n = 24)	
Cardiovascular chronic drug therapy						
ACE inhibitors or ARB	8 (5.8)	6 (6.3)	0	0	2 (8.3)	.898
Beta-blocker	2 (1.4)	1 (1.0)	0	1 (9.1)	0	.284
Statin	17 (12.2)	16 (16.7)	0	1 (9.1)	0	.085
Antiplatelet	5 (3.6)	5 (5.2)	0	0	0	.802
Anticoagulant	4 (2.9)	3 (3.1)	0	1 (9.1)	0	.547
Treatment during SARS-CoV-2 infection						
Required hospitalization	23 (16.5)	19 (19.8)	1 (12.5)	2 (18.2)	1 (4.2)	.281
Oxygen therapy	15 (10.8)	13 (13.5)	0	1 (9.1)	1 (4.2)	.546
Paracetamol	124 (89.2)	86 (89.6)	6 (75.0)	9 (81.8)	23 (95.8)	.218
Ibuprofen	17 (12.2)	11 (11.5)	1 (12.5)	4 (36.4)	1 (4.2)	.068
Azithromycin	57 (41.0)	39 (40.6)	4 (50.0)	5 (45.5)	9 (37.5)	.899
Hydroxychloroquine	33 (23.7)	26 (27.1)	2 (25.0)	3 (27.3)	2 (8.3)	.236
Lopinavir-ritonavir	17 (12.2)	14 (14.6)	1 (12.5)	1 (9.1)	1 (4.2)	.56
Oral glucocorticoids	9 (6.5)	4 (4.2)	1 (12.5)	2 (18.2)	2 (8.3)	.123
High-dose intravenous glucocorticoids*	15 (10.8)	12 (12.5)	1 (12.5)	1 (9.1)	1 (4.2)	.723
Interleukin-6 inhibitors (tocilizumab, siltuximab)	18 (12.9)	14 (14.6)	1 (12.5)	2 (18.2)	1 (4.2)	.465
Interleukin-1 inhibitor (anakinra)	2 (1.4)	2 (2.1)	0	0	0	1.000
Additional drug therapy on examination						
Inhaled glucocorticoids	5 (3.6)	4 (4.2)	0	0	1 (4.2)	1.000
Oral glucocorticoids	2 (1.4)	1 (1.0)	0	1 (9.1)	0	.284

	All participants	Presence of pericardial and myocardial manifestations				*P*
	(N = 139)	No (n = 96)	Pericarditis (n = 8)	Myopericarditis (n = 11)	Myocarditis (n = 24)	
Low-molecular weight heparin	4 (2.9)	3 (3.1)	0	1 (9.1)	0	.547

ACE, angiotensin-converting enzyme; ARB, angiotensin receptor blocker.

The data are expressed as No. (%).

*High-dose intravenous glucocorticoids was considered when at least a bolus of methylprednisolone of 250 mg was administered.

P value for comparison among the 4 participants groups.

Table 2 of the supplementary data

Electrocardiographic measures

	All participants	Presence of pericardial and myocardial manifestations				*P*
	(N = 139)	No (n = 96)	Pericarditis (n = 8)	Myopericarditis (n = 11)	Myocarditis (n = 24)	
Sinus rhythm	139 (100)	96 (100)	8 (100)	11 (100)	24 (100)	.999
Sinus tachycardia over 100 bpm	2 (1.4)	2 (2.1)	0	0	0	.999
Sinus bradycardia under 50 bpm	5 (3.6)	3 (3.1)	0	0	2 (8.3)	.650
Extrasystole	2 (1.4)	2 (2.1)	0	0	0	.999
Atrioventricular block or bundle branch block	9 (6.5)	7 (7.3)	0	0	2 (8.3)	1.000
Intraventricular conduction delay	15 (10.8)	13 (13.5)	1 (12.5)	0	1 (4.2)	.413
ST-segment depression or T-wave inversion	23 (16.5)	17 (17.7)	1 (12.5)	1 (9.1)	4 (16.7)	.972
New Q waves	0	0	0	0	0	.999
Long-QT interval[*]	5 (3.6)	4 (4.2)	0	1 (9.1)	0	.572
Low voltages	5 (3.6)	2 (2.1)	1 (12.5)	1 (9.1)	1 (4.2)	.142
Early repolarization	8 (5.8)	7 (7.3)	0	0	1 (4.2)	.999
Electrocardiographic pericarditis-like changes						
Widespread ST-elevation	13 (9.4)	8 (8.3)	2 (25.0)	3 (27.3)	0	.018
PR depression	33 (23.7)	19 (19.8)	5 (62.5)	5 (45.5)	4 (16.7)	.014

The data are expressed as No. (%).

[*]Long-QT interval was defined as a rate-corrected (Bazett) QT interval exceeding 450 milliseconds in males and 460 milliseconds in females.

P value for comparisons among the 4 participants groups.

Table 3 of the supplementary data

Electrocardiographic findings in participants with electrocardiographic abnormalities on study examination and prior baseline electrocardiogram at the time of being hired at the hospital

	Baseline electrocardiogram (n = 53)	Study electrocardiogram (n = 53)	*P*	
Sinus rhythm	53 (100)	53 (100)	.999	
Sinus tachycardia over 100 bpm	1 (1.9)	2 (3.8)	.999	
Sinus bradycardia under 50 bpm	1 (1.9)	4 (7.5)	.363	
Extrasystole	0	1 (1.9)	.495	
AV block or bundle branch block	1 (1.9)	3 (5.7)	.618	
Intraventricular conduction delay	12 (22.6)	14 (26.4)	.822	
ST-segment depression or T-wave inversion	1 (1.9)	16 (30.2)	< .001	
New Q waves	0	0	.999	
Long-QT interval[*]	0	2 (3.8)	.495	
Low voltages	0	3 (5.7)	.243	
Early repolarization	2 (3.8)	3 (5.7)	.999	
Pericarditis-like changes				
Widespread ST elevation	0	13 (24.5)	< .001	
PR depression	0	28 (52.8)	< .001	

Data are expressed as No. (%).

*Long-QT interval was defined as a rate-corrected (Bazett) QT interval exceeding 450 milliseconds in men and 460 milliseconds in women.

P value for comparison among the 4 participants groups.

Table 4 of the supplementary data

Left ventricular myocardial T_1-relaxation time, T_1-extracellular volume, and T_2-relaxation time reference ranges extracted from the population-based controls

Controls	Native T_1-relaxation time (msec)				T_1-extracellular volume (%)				T_2-relaxation time (msec)			
Segment	Mean	SD	95%CI (sup-inf)		Mean	SD	95%CI (sup-inf)		Mean	SD	95%CI (sup-inf)	
1	1017.4	31.7	1079.5	955.3	25.6	3.3	32.0	19.1	51.5	5.6	62.5	40.6
2	1007.9	39.9	1086.1	929.6	26.0	2.9	31.7	20.3	49.7	7.6	64.5	34.8
3	1013.0	35.1	1081.8	944.3	26.5	2.5	31.4	21.6	48.8	4.7	58.0	39.6
4	1023.1	37.0	1095.7	950.6	26.9	3.1	32.9	20.8	49.3	5.4	59.9	38.8
5	1042.0	32.0	1104.8	979.2	25.6	2.7	30.9	20.2	50.5	7.1	64.4	36.5
6	1023.2	34.7	1091.3	955.2	24.9	2.8	30.4	19.3	46.6	8.6	63.4	29.8
7	1003.7	38.0	1078.2	929.2	26.3	3.6	33.4	19.2	47.2	8.0	62.8	31.5
8	1009.7	44.5	1096.9	922.6	26.8	3.1	32.9	20.7	52.4	7.4	66.8	38.0
9	1017.9	41.4	1099.1	936.8	26.8	3.2	33.1	20.4	51.6	5.7	62.7	40.5
19	1026.7	41.3	1107.7	945.7	26.0	3.4	32.7	19.3	51.3	6.5	64.0	38.6
11	1024.8	38.9	1101.0	948.6	25.2	2.8	30.6	19.8	53.0	5.9	64.5	41.6
12	1023.0	41.4	1104.1	941.8	25.3	2.7	30.6	20.0	49.9	8.1	65.8	34.0
13	1011.1	41.6	1092.7	929.6	26.9	2.9	32.6	21.2	50.0	7.2	64.1	35.8
14	1025.8	45.7	1115.5	936.2	27.3	3.5	34.0	20.5	52.1	7.5	66.8	37.5
15	1021.4	56.5	1132.2	910.6	25.7	3.9	33.4	17.9	53.0	6.3	65.3	40.8
16	1017.6	57.3	1129.9	905.2	25.7	3.5	32.6	18.8	51.9	5.4	62.5	41.4

95%CI, 95% confidence interval; SD, standard deviation; sup, superior; inf, inferior.

Table 5 of the supplementary data

Interpretable segments of all possible for T_1-relaxation time, T_1-extracellular volume, and T_2-relaxation time

	Interpretable segments	All segments	Percentage of analyzed segments
T_1-relaxation time	1963	2224	88.3
T_1-extracellular volume	1933	2224	86.9
T_2-relaxation time	2076	2224	93.3

Of all 2224 segments (16 segments per patient x 139 patients), increased T_2-relaxation time was noted in 12 segments out of 2076 (0.6%), T_2-weighted hyperintensity in 45 segments out of 2224 (2.0%), increased T_1-relaxation time in 102 segments out of 1963 (5.2%), T_1-extracellular volume in 213 segments out of 1933 (11.0%), and T_1-LGE in 21 segments out of 2224 (0.9%). Edema and fibrotic areas had a subepicardial only distribution, or a subepicardial to mid-wall distribution, with sparing of endocardium and subendocardium in all patients. Overall T_1 and extracellular volume segments read were 88.3% and 86.9% respectively (T_1 native basal short-axis slice 97.1%, mid 96.7%, and apical 62.2%). Overall T_2 segments read 93.3% (basal short-axis slice 91.5%, mid 95.6%, and apical 92.8%). The highest percentage of segments rejected were at the apical level. Only 2 of 35 patients with myocarditis/myopericarditis were diagnosed based on apical segment values.

Table 6 of the supplementary data

Baseline characteristic and on examination for participants testing positive for SARS-CoV-2 by RT-PCR or by anti-SARS-CoV-2-IgG antibodies.

	RT-PCR (n = 103)	Anti-SARS-CoV-2-IgG (n = 36)	*P*
Age, y	52 [43–58]	50 [39–56]	.245
Female sex	70 (68.0)	30 (83.3)	.088
Health care worker category			.001
Medical staff	31 (30.1)	4 (11.1)	
Nurse	41 (39.8)	8 (22.2)	
Other	31 (30.1)	24 (67.7)	
Direct attention to COVID-19 patients	44 (42.7)	23 (63.9)	.034
Coexisting conditions			
Obesity[a]	11 (10.7)	6 (16.7)	.559
Hypertension	14 (13.6)	3 (8.3)	.559
Diabetes	1 (1.0)	1 (2.8)	.452
Dyslipidaemia	22 (21.4)	5 (13.9)	·464
Current smoking	5 (4.9)	1 (2.8)	.999
Past smoking	50 (48.5)	20 (55.6)	.562
Alcohol use[b]	19 (18.4)	4 (11.1)	.436
Cardiovascular disease	6 (5.8)	2 (5.6)	.999
Pulmonary disease[c]	6 (5.8)	2 (5.6)	.999
Sleep apnoea-hypopnea syndrome	8 (7.8)	0	.112
Chronic kidney disease	3 (2.9)	2 (5.6)	.604
Cancer	3 (2.9)	1 (2.8)	.999
Al least 1 of the above	78 (75.7)	28 (77.8)	.999
Symptoms at SARS-CoV-2 infection			

	RT-PCR (n = 103)	Anti-SARS-CoV-2-IgG (n = 36)	*P*
Number of symptoms	8 [5-10]	5 [3-7]	.001
General			
Fatigue	87 (84.5)	30 (83.3)	.999
Fever	81 (78.6)	13 (36.1)	< .001
Cough	70 (68.0)	21 (58.3)	.314
Headache	68 (66.0)	22 (61.1)	.686
Myalgia	67 (65.0)	16 (44.4)	.047
Anosmia	61 (59.2)	12 (33.3)	.011
Ageusia	52 (50.5)	14 (38.9)	.251
Abdominal pain or diarrhoea	54 (52.4)	10 (27.8)	.012
Chills	52 (50.5)	8 (22.2)	.003
Score throat	42 (40.8)	13 (36.1)	.695
Nausea or vomiting	24 (23.3)	6 (16.7)	.361
Clumsiness	17 (16.5)	3 (8.3)	.281
Memory loss	15 (14.6)	4 (11.1)	.780
Skin lesions	4 (3.9)	1 (2.8)	.999
Cardiac			
Shortness of breath	53 (51.5)	15 (41.7)	.339
Palpitations	33 (32.0)	11 (30.6)	.999
Chest pain	31 (30.1)	9 (25.0)	.671
Dizziness	3 (2.9)	1 (2.8)	.999
At least 1 cardiac symptom	66 (64.1)	20 (55.6)	.427
Covid-19 confirmed pneumonia	26 (25.2)	1 (2.8)	.003
Cardiovascular chronic drug therapy			
ACE inhibitors or ARB	6 (5.8)	2 (5.6)	.999

	RT-PCR (n = 103)	Anti-SARS-CoV-2-IgG (n = 36)	*P*
Beta-blocker	2 (1.9)	0	.999
Statin	13 (12.6)	4 (11.1)	.999
Antiplatelet	5 (4.9)	0	.327
Anticoagulant	4 (3.9)	0	.572
Treatment at SARS-CoV-2 infection			
Required hospitalization	22 (21.4)	1 (2.8)	.008
Oxygen therapy	14 (13.6)	1 (2.8)	.115
Paracetamol	95 (92.2)	29 (80.6)	.065
Ibuprofen	12 (11.7)	5 (13.9)	.770
Azithromycin	54 (52.4)	3 (8.3)	< .001
Hydroxychloroquine	32 (31.1)	1 (2.8)	< .001
Lopinavir-ritonavir	16 (15.5)	1 (2.8)	.072
Oral glucocorticoids	9 (8.7)	0	.111
High-doses intravenous glucocorticoids[d]	14 (13.6)	1 (2.8)	.115
Interleukin-6 inhibitors (tocilizumab, siltuximab)	17 (16.5)	1 (2.8)	.042
Interleukin-1 inhibitor (anakinra)	2 (1.9)	0	.999
Additional drug therapy at examination			
Inhaled glucocorticoids	5 (4.9)	0	.327
Oral glucocorticoids	2 (1.9)	0	.999
Low-molecular weight heparin	4 (3.9)	0	.572
Vital signs on examination			
Blood pressure, mmHg			
Systolic	125 [113-140]	122 [113-137]	.883
Diastolic	76 [70-82]	75 [69-84]	.899

	RT-PCR (n = 103)	Anti-SARS-CoV-2-IgG (n = 36)	*P*
Heart rate, bpm	71 [63-80]	69 [63-79]	.686
Oxygen saturation < 95%	7 (6.8)	3 (8.3)	.719
Physical examination			
Pericardial rub	0	0	.999
Heart murmur	2 (1.9)	1 (2.8)	.999
Third and fourth heart sound	0	0	.999
Pulmonary crackles	4 (3.9)	1 (2.8)	.999
Symptoms on examination			
No symptoms	30 (29.1)	18 (50.0)	.027
General			
Fatigue	33 (32.0)	4 (11.1)	.016
Anosmia	9 (8.7)	3 (8.3)	.999
Ageusia	5 (4.9)	2 (5.6)	.999
Headache	6 (5.8)	1 (2.8)	.677
Sore throat	6 (5.8)	1 (2.8)	.677
Abdominal pain	4 (3.9)	2 (5.6)	.649
Memory loss	4 (3.9)	0	.572
Join pain	3 (2.9)	0	.568
Piloerection	2 (1.9)	0	.999
Cardiac			
Dyspnoea or shortness of breath	28 (27.2)	8 (22.2)	.661
Chest pain	21 (20.4)	6 (16.7)	.807
Pericarditis-like	16 (15.5)	2 (5.6)	.157
Palpitations	17 (16.5)	3 (8.3)	.281
Dizziness	5 (4.9)	3 (8.3)	.427

	RT-PCR (n = 103)	Anti-SARS-CoV-2-IgG (n = 36)	*P*
At least 1 cardiac symptom	44 (42.7)	14 (38.9)	.845

ACE, angiotensin-converting enzyme; ARB, angiotensin receptor blocker.

The data are expressed as No. (%) and median [interquartile range].

[a] Obesity was considered if body-mass index of 30 or more.

[b] Alcohol use was considered an average of at least 1 drink a day.

[c] All participants with previous pulmonary disease reported asthma.

[d] High-doses intravenous glucocorticoids was considered when at least a bolus of methylprednisolone of 250 mg was administered. *P* value for comparison among both groups.

Table 7 of the supplementary data

Distribution of subsets of myeloid immune cells in blood.

	Healthy donors (n = 463)	All participants (N = 139)	*P*	Presence of pericardial and myocardial manifestations				*P*
				No (n = 96)	Pericarditis (n = 8)	Myopericarditis (n = 11)	Myocarditis (n = 24)	
Neutrophils	3723 [2969-4613]	3430 [2633-4225]	0.010	3468 [2647-4223]	3013 [2385-3699]	3966 [3157-4255]	3023 [1966-4208]	.491
% cases ↓ 5th p/ ↑ 95th p	-	18 (12.9)/5 (3.6)	< .001/.001	10 (10.4)/4 (4.2)	1 (12.5)/0	0/0	7 (29.2)/1 (4.2)	.051 / .844
MDSC-like neutrophils	6 [2-13]	2 [1-5]	.550	2.9 [1.3-7.6]	2 [0.4-5]	2 [1-3]	2 [1-4]	.625
Immature $CD16^{-}CD62L^{-}$	5 [2-9]	2 [0.8-4]	.563	2 [0.9-6]	1 [0.4-4]	2 [0.6-2]	2 [0.9-3]	.604
Immature $CD16^{-}CD62L^{+}$	0.6 [0.2-1]	0.5 [0.2-1]	.677	0.7 [0.3-1]	0.5 [0.1-1]	0.4 [0.2-0.7]	0.4 [0.2-0.7]	.840
Eosinophils	157 [101-249]	74 [47-149]	< .001	82 [50-130]	48 [31-189]	59 [46-69]	102 [39-191]	.463
% cases ↓ 5th p/ ↑ 95th p	-	38 (27.3)/1 (0.7)	< .001/.231	24 (25.0)/1 (1.0)	4 (50.0)/0	3 (27.3)/0	7 (29.2)/0	.499 / .929
Basophils	38 [21-52]	47 [35-62]	.007	49 [37-62]	34 [23-55]	36 [29-56]	51 [38-65]	.293
% cases ↓ 5th p/ ↑ 95th p	-	4 (2.9)/5 (3.6)	< .001/< .001	2 (2.1)/3 (3.2)	1 (12.5)/1 (25)	1 (9.1)/1 (9.1)	0/1 (4.2)	.169 / .719
Monocytes	317 [245-433]	405 [328-523]	< .001	418 [345-533]	369 [307-424]	404 [347-476]	358 [282-574]	.724
% cases ↓ 5th p/ ↑ 95th p	-	3 (2.2)/8 (5.8)	.012/ < .001	3 (3.1)/5 (5.2)	0/ 1 (12.5)	0/0	0/2 (8.3)	.712 / .639
Classical monocytes	271 [210-355]	342 [267-437]	.005	357 [289-447]	298 [319-669]	386 [264-413]	297 [210-437]	.592
$CD62L^{+}$ $FcεRI^{+}$	31 [5-48]	14 [3-59]	.911	18 [5-61]	4 [1-95]	1 [0.5-35]	11 [5-46]	.914
$CD62L^{+}$ $FcεRI^{-}$	140 [90-183]	234 [161-345]	< .001	242 [160-369]	291 [248-513]	249 [50-350]	182 [157-244]	.304
$CD62L^{-}$ $FcεRI^{+}$	5 [1-22]	2 [0.3-7]	.935	2 [0.3-7]	0.4 [0.1-3]	2 [0.1-10]	4 [0.4-10]	.424
$CD62L^{-}$ $FcεRI^{-}$	69 [36-176]	42 [23-77]	< .001	41 [20-79]	34 [22-42]	69 [37-117]	49 [32-75]	.704
Intermediate monocytes	14 [10-20]	15 [10-19]	.865	15 [10-21]	13 [4-17]	13 [8-18]	16 [10-19]	.745
Nonclassic monocytes	33 [25-42]	43 [32-63]	.003	43 [32-67]	39 [35-52]	42 [33-69]	43 [29-60]	.897
Dendritic cells	29 [20-35]	28 [20-35]	.561	28 [20-35]	28 [20-33]	29 [18-42]	23 [19-35]	.920
% cases ↓ 5th p/ ↑ 95th p	-	14 (10.2)/5 (3.6)	< .001/< .001	11 (11.7)/5 (5.3)	0/0	1 (9.1)/0	2 (8.3)/0	.755 / .508
MDSC	0 [0-1.1]	0.8 [0.3-1.4]	.311	0.8 [0.3-1.7]	0.5 [0.4-0.8]	0.8 [0.5-1.4]	0.8 [0.3-1.3]	.212

	Healthy donors (n = 463)	All participants (N = 139)	*P*	Presence of pericardial and myocardial manifestations				*P*
				No (n = 96)	Pericarditis (n = 8)	Myopericarditis (n = 11)	Myocarditis (n = 24)	
Myeloid dendritic cells	18 [14-26]	19 [14-26]	.180	19 [14-25]	20 [16-26]	22 [13-29]	16 [13-28]	.953
CD1c$^+$ m dendritic cells	17 [14-25]	19 [14-25]	.210	19 [13-25]	19 [15-26]	20 [13-27]	15 [13-24]	.755
CD141$^+$ m dendritic cells	1 [0.6-1]	0.9 [0.6-1]	.284	0.9 [0.6-1]	0.6 [0.5-1]	0.8 [0.7-2]	0.6 [0.5-1]	.227
Plasmacytoid dendritic cells	8 [6-11]	6 [4-9]	.205	6 [5-10]	6 [1-11]	7 [5-8]	6 [4-8]	.816
Axl$^+$ dendritic cells	0.3 [0.2-0.4]	0.3 [0.2-0.5]	.271	0.3 [0.2-0.5]	0.2 [0.1-0.4]	0.3 [0.2-0.5]	0.3 [0.2-0.5]	.408

MDSC, myeloid-derived suppressor cells, m, myeloid.

The data are expressed as median [interquartile range] of cells/µL of blood or No. (%) of cases lower than the 5th percentile (↓5thp) and higher than 95th percentile (↑95thp) for each cell subset in age-matched healthy donors. Left *P* value for comparisons between healthy donors vs all participants. Right *P* value for comparison among the 4 participant groups. Comparisons between healthy donors vs all participants are adjusted for age and sex.

Table 8 of the supplementary data

Distribution of the major subsets of lymphoid cells in blood

	Healthy donors (n = 463)	All participants (N = 139)	*P*	Presence of pericardial and myocardial manifestations				*P*
				No (n = 96)	Pericarditis (n = 8)	Myopericarditis (n = 11)	Myocarditis (n = 24)	
Lymphocytes	1675 [1332-2223]	2221[1717-2563]	< .001	2294 [1854-2760]	1990 [1555-2422]	1660 [1379-2089]	1998 [1619-2439]	.055
% cases ↓ 5thp/ ↑ 95thp	-	3 (2)/8 (6)	.012/< .001	1 (1.0)/6 (6.3)	1 (12.5)/1 (12.5)	1 (9.1)/0	0/1 (4.2)	.054 /.683
T cells	1246 [943-1642]	1652 [1348-1985]	< .001	1747 [1417-2003]	1417 [1194-1938]	1350 [1186-1621]	1635 [1309-2018]	.102
% cases ↓5thp/↑95thp	-	1 (1)/10 (7)	.231/< .001	0/8 (8.3)	0/1 (12.5)	1 (9.1)/0	0/1 (4.2)	.304 / .636
CD4+ T cells	716 [567-961]	1017 [791-1263]	< .001	1041 [817-1273]	867 [836-1011]	841 [719-902]	1071 [711-1332]	.066
% cases ↓ 5thp/ ↑ 95thp	-	1 (1)/14 (10)	.231/< .001	0/11 (11.5)	0/1 (12.5)	1 (9.1)/0	0/2 (8.3)	.304 / .667
CD8+ T cells	407 [291-590]	507 [388-696]	< .001	541 [392-751]	383 [338-788]	452 [335-556]	529 [413-647]	.592
% cases ↓5thp/↑95thp	-	0/9 (6.5)	-/< .001	0/7 (7.3)	0/1 (12.5)	0/0	0/1 (4.2)	– / .669
CD4^{-}CD8^{-lo} T cells	46 [28-79]	78 [48-130]	< .001	88 [48-133]	104 [64-157]	71 [64-77]	67 [37-111]	.456
% cases ↓5thp/↑95thp	-	5 (3.6)/24 (17.3)	.003/< .001	4 (4.2)/17 (17.7)	1 (12.5)/2 (25.0)	0/1 (9.1)	0/4 (16.7)	.385 / .833
CD4^{-}CD8^{-lo}T□□ cells	26 [15-36]	21 [14-33]	.892	22 [14-37]	29 [14-41]	21 [15-25]	17 [11-28]	.448
% cases ↓5thp/↑95thp	-	7 (5.0)/10 (7.2)	< .001/< .001	5 (5.2)/8 (8.3)	2 (25.0)/0	0/0	0/2 (8.3)	.036 / .636
T□□ cells	56 [33-107]	52 [31-93]	.609	59 [32-93]	76 [40-128]	49 [38-58]	46 [22-73]	.610
% cases ↓5thp/↑95thp	-	2 (1.4)/8 (5.8)	.053/< .001	2 (2.1)/7 (7.3)	0/1 (12.5)	0/0	0/0	.823 / .499
NK cells	260 [162-372]	213 [137-321]	.427	237 [143-337]	233 [142-281]	120 [76-321]	156 [137-248]	.230
% cases ↓5thp/↑95thp	-	9 (6.5)/6 (4.3)	< .001/0.001	5 (5.2)/5 (5.2)	0/0	3 (27.3)/0	1 (4.2)/1 (4.2)	.003 / .791
B cells	154 [108-228]	208 [158-297]	< .001	234 [175-327]	233 [119-443]	174 [153-188]	181 [136-230]	.020
% cases ↓5thp/↑95thp	-	2 (1.4)/16 (11.5)	.053/< .001	1 (1.0)/10 (12.5)	1 (12.5)/2 (25.0)	0/0	0/2 (8.3)	.525 / .362
Plasma cells	2 [0.8-3]	0.8 [0.3-2]	< .001	0.9 [0.5-2]	1 [0.2-1]	0.4 [0.3-0.8]	1 [0.3-2]	.362

	Healthy donors (n = 463)	All participants (N = 139)	*P*	Presence of pericardial and myocardial manifestations				*P*
				No (n = 96)	Pericarditis (n = 8)	Myopericarditis (n = 11)	Myocarditis (n = 24)	
% cases ↓5thp/↑95thp	-	11 (7.9)/1 (0.7)	< .001/.231	7 (7.3)/1 (1.0)	0/0	2 (18.2)/0	2 (8.3)/0	.506 / .929

NK, natural killer.

The data are expressed as the median [interquartile range] of cells/µL of blood or No. (%) of cases lower than the 5th percentile (↓5thp) and higher than the 95th percentile (↑95thp) for each cell subset in age-matched healthy donors. Left *P* value for comparisons between healthy donors vs all participants. Right *P* value for comparison among the 4 participant groups. Comparisons between healthy donors vs all participants are adjusted for age and sex.

Figure 1 of the supplementary data. An example of electrocardiographic pericarditis-like changes. Widespread ST elevation and PR depression is observed.

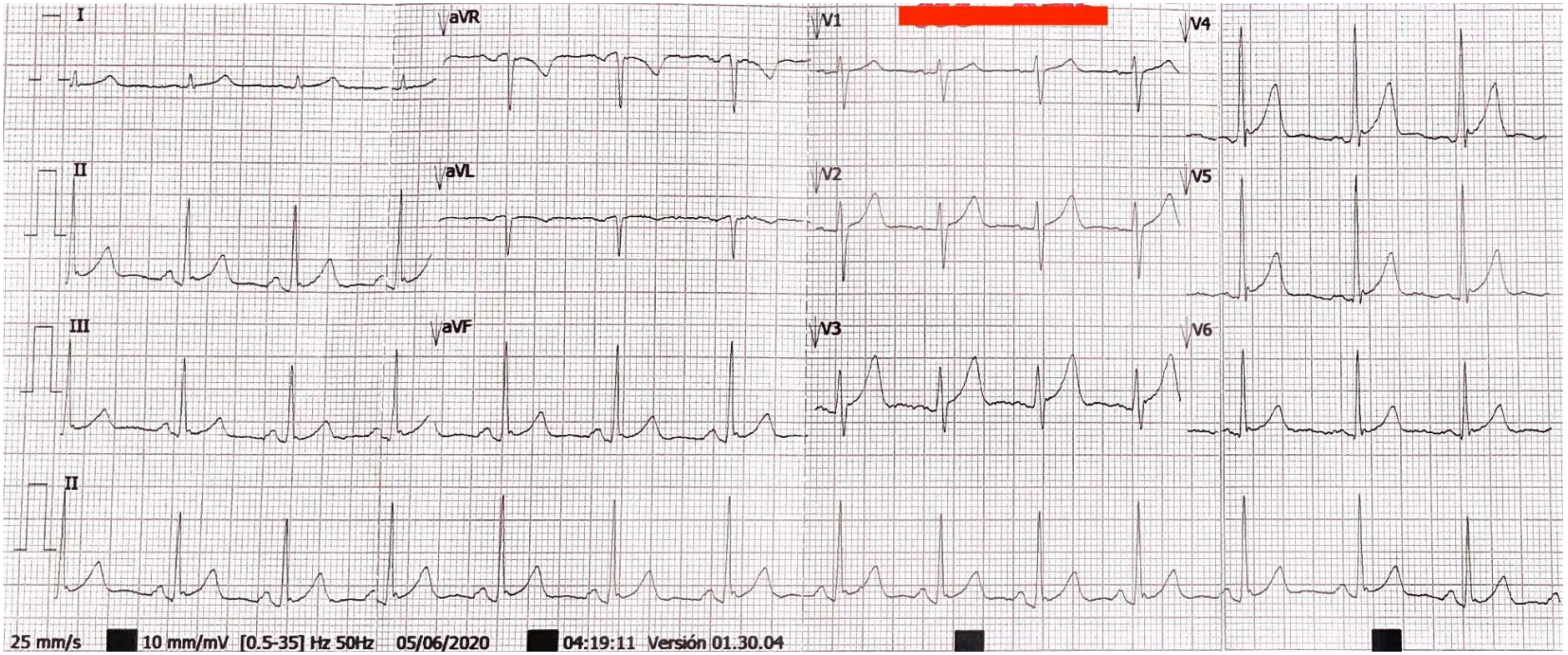

LISTADO DE INVESTIGADORES

The following investigators participated in the CCC (Cardiac Covid-19 health care workers) study:

Cardiology Department, University Hospital of Salamanca, IBSAL, Salamanca, Spain: Pedro L Sánchez, Rocío Eiros, Manuel Barreiro-Pérez, Ana Martín-García, Eduardo Villacorta, Soraya Merchán, Clara Sánchez-Pablo, David González-Calle, Inés Toranzo, Elena Díaz-Peláez, Laura Macías-Álvarez, Nuria Sánchez-Barbero, Ana Moralejo-Salinas, Leticia Vicente-Pacho, Pedro Vara-González, Juan Carlos Castro-Garay, Pablo Luengo Modéjar, P. Ignacio Dorado-Díaz, and Alberto García-Galindo.

Occupational Health Service, University Hospital of Salamanca, IBSAL, Salamanca, Spain: José L Bravo-Grande, M Asunción Blanco-González, Elena Alonso-Vicente, Patricia Arranz-Vaquero.

Translational and Clinical Research Program, Centro de Investigación del Cáncer (CIC) Instituto de Biología Molecular y Celular del Cancer (IBMCC), IBSAL, Salamanca, Spain: Alberto Orfao, Julia Almeida, Alba Pérez-Pons, Alba Torres-Valle, Oihane Pérez-Escurza, Blanca Fuentes-Herrero, Guillermo Oliva-Ariza, Quentin Lecrevisse, Rafael Fluxa, Martín Pérez-Andrés, Vitor Botafogo Gonçalves, Daniela Damasceno, and Francisco Javier Morán-Plata.

CONFLICTS OF INTEREST

M. Pérez-Andrés, V. Botafogo y D. Damasceno report being one of the inventors on the EuroFlow-owned European patent 119646NL00 registered in November 2019 (Means and methods for multiparameter flow cytometry based leukocyte subsetting).

Pedro L Sánchez as corresponding author confirms that the entire list of investigators is in agreement with the content of the manuscript and its submission to *Revista Española de Cardiología.*